Numerical study of extreme events in a laser diode with phase-conjugate optical feedback

Émeric Mercier,* Armelle Even, Elodie Mirisola, Delphine Wolfersberger, and Marc Sciamanna
OPTEL Research Group, Laboratoire Matériaux Optiques, Photonique et Systèmes, EA No. 4423, CentraleSupélec, 2 Rue Édouard Belin, 57070 Metz, France

(Received 27 October 2014; published 24 April 2015)

Extreme intensity pulses sharing statistical properties similar to rogue waves have been recently observed in a laser diode with phase-conjugate feedback [A. Karsaklian Dal Bosco, D. Wolfersberger, and M. Sciamanna, Opt. Lett. **38**, 703 (2013)], but remain unexplained. We demonstrate here that a rate equation model of a laser diode that includes an instantaneous phase-conjugate feedback field reproduces qualitatively well the statistical features of these extreme events as identified in the experiment, i.e., the deviation of the intensity statistics to a Gaussian-shape statistics and the statistics of the time separating extreme events. The numerical simulations confirm the importance of the feedback strength in increasing the number of such extreme events and allow us to explain how extreme events emerge from a sequence of bifurcations on self-pulsating solutions, the so-called external cavity modes.

DOI: 10.1103/PhysRevE.91.042914 PACS number(s): 05.45.−a, 42.65.Sf, 42.55.Px, 42.65.Hw

I. INTRODUCTION

The impact of optical feedback on the dynamics of a semiconductor laser diode has been extensively studied over the past 40 years. Several beneficial effects have been identified such as a narrowing of the wavelength of emission or a reduction of the lasing threshold [1]. On the downside, however, the laser diode typically deviates from its otherwise steady-state operation and a large variety of nonlinear dynamics including self-pulsation and chaos has been identified. One way of classifying the richness of the dynamical behavior is to consider whether the time delay induced by the external feedback is small or large with respect to the laser diode relaxation oscillation period, hence referring to a short or long external cavity, respectively [2]. In the case of a long external cavity, chaotic dynamics, referred to as coherence collapse [3] and a low-frequency fluctuation (LFF) regime [4], are typically observed when increasing the feedback strength. Low-frequency fluctuation has been shown to originate from chaotic itinerancy among destabilized external-cavity modes [5]. In the case of a short external cavity, dynamics typically consist of self-pulsation from mode beating between external-cavity modes [6,7] or quasiperiodic regular pulse packages [8,9] with the slow modulation of pulsing dynamics at the external-cavity frequency. Apart from the time-delay value, the richness of the observed dynamics depends on the type of optical feedback. While studies have addressed in detail conventional optical feedback (COF) from a distant mirror, optoelectronic feedback [10,11], and incoherent feedback [12], much less work has been published regarding phase-conjugate optical feedback (PCF) [13–16].

Although at first sight chaotic dynamics from a laser diode with COF share several properties with those arising from PCF [15], a closer inspection of the underlying bifurcations unveils significant differences. For example, except for very low feedback strength, there is no steady-state external-cavity mode (ECM) in the case of PCF. Instead, ECMs are self-pulsating solutions at a frequency being a multiple of the external-cavity frequency [16,17]. These superharmonic self-pulsating solutions have only recently been found in experiment [18]. As recently shown theoretically [19], secondary bifurcations on these limit-cycle ECM solutions explain the occurrence of LFFs as observed experimentally [20].

In this paper we focus on a specific dynamic of a laser diode with PCF, which consists of extremely-high-intensity pulses that exhibit statistical properties similar to those observed in so-called rogue waves [21]. Rogue waves are inspired from oceanographic studies [22] and are rare and high-amplitude waves that appear randomly at the surface of an otherwise calm sea. Rogue waves were first observed in optics in nonlinear propagation of light launched in an optical fiber showing a supercontinuum [23]. The concept of optical rogue waves was then generalized to include the study of extreme events in optics where a variation of a parameter leads to a deviation of the intensity statistics to the otherwise Gaussian distribution, hence explaining the occurrence of rare and intense pulses. Even though rogue waves and extreme events are different in nature, they may share statistical properties owing to the fact that they both correspond to large deviations of the system state away from its nominal value [24]. Examples of rogue waves and extreme events include high-intensity pulses underlying chaotic dynamics in laser diodes with optical injection [25,26] or optical feedback [21,27], and high-amplitude localized light peaks in the transverse plane of a spatially extended nonlinear optical cavity [28–30]. Our purpose is here to provide a theoretical framework to explain the emergence of these extreme events in a laser diode with PCF. More specifically, we show that a rate-equation model, inspired by Lang and Kobayashi equations [31] and adapted to the case of PCF [16], is able to reproduce the dynamical features observed in the experiment [21]. Of particular interest is the influence of the delay and the feedback rate (a measure of the quantity of light that is fed back in the laser) on the number and statistics of time separating extreme events. Not only are the theoretical results in good qualitative agreement with the experimental observations, but they also allow us to provide insight into the physics underlying the emergence of extreme events. We indeed demonstrate that extreme events emerge from secondary bifurcations on the ECMs of the PCF laser

*Corresponding author: emeric.mercier@supelec.fr

system. Most importantly, we identify the parameter range where extreme events are detected and relate the occurrence of extreme events to the occurrence of chaos crisis in the bifurcation cascade leading to ECM solutions. Finally, we explain why the number of extreme events is found to increase when increasing the feedback strength in the PCF laser system.

This paper is organized as follows. Section II focuses on the description of the rate-equation model we use. Section III demonstrates good qualitative agreement between numerical simulations of this model and characteristic dynamics recently observed experimentally for different values of the external-cavity length and hence of the time delay. In Sec. IV we analyze a case of intermediate value of the external-cavity time delay with low to moderate feedback strength where extreme events appear with a significant deviation of the intensity statistics from a Gaussian distribution. We focus on the evolution of the distribution of extrema, the analysis of the time between said extreme events, how these time intervals are distributed according to a log-Poisson law, and how these extreme events emerge from chaos. Finally, Sec. V presents a summary of our study and our conclusions.

II. RATE-EQUATION MODEL

The model we use is a set of rate equations adapted to the case of PCF from the Lang and Kobayashi equations [31] where quantities, including time, are normalized [16,17,19]:

$$\frac{dY}{dt} = (1 + i\alpha)ZY + \gamma Y^*(t - \theta), \tag{1}$$

$$T\frac{dZ}{dt} = P - Z - (1 + 2Z)|Y|^2, \tag{2}$$

where Y is the complex slowly varying envelope of the electric field and Z is the carrier density. These quantities are normalized, along with time, which is normalized by the photon lifetime $\tau_p = 1.4$ ps. Here α is the linewidth enhancement factor, γ is the normalized feedback rate, θ is the normalized delay, T is the ratio of the carrier to photon lifetimes, and P represents the pumping current above threshold. The model matches recent experimental conditions [18,20,21] since it considers the realization of a phase-conjugate mirror through self-pumped four-wave mixing, thus inducing no detuning in the feedback term [32]. For the sake of simplicity, we will consider here that the response from the mirror is instantaneous, hence neglecting the time scale of the nonlinear optical process that yields phase conjugation [33].

We consider the following set of parameter values: $\alpha = 4$, $T = 1428$, and $P = 0.0417$, as is common for several other previous theoretical studies [14,16,17,34]. In addition, γ and θ will be our free parameters, which we change to reproduce the different types of dynamics and to influence the properties of said dynamics. Indeed, recent experiments on PCF [18,20,21] have shown that both the time delay and the feedback strength play a crucial role on the bifurcations and on the waveforms of the observed dynamics. In addition, this paper aims at justifying theoretically the experimental observations of Ref. [21], where the feedback strength was considered as the experimentally varying parameter.

III. FROM SELF-PULSATION TO CHAOTIC DYNAMICS

The equations are numerically integrated with a fourth-order Runge-Kutta algorithm with a fixed step $h = 1$ in normalized time, which corresponds to a step of $\tau_p = 1.4$ ps in real time. The time step has been chosen small enough so as to ensure the numerical convergence of the results. Unless specified otherwise, the time traces present the optical output power filtered using a moving-average filter with a 3-dB frequency cut of 4 GHz so as to account for the limited bandwidth of the acquisition in the experimental setup of Refs. [18,20,21]. The radio-frequency (rf) spectra have been made using a fast Fourier transform on unfiltered time traces.

Figure 1 presents simulated time traces of three typical dynamics that qualitatively match experimental observations in a laser diode with phase-conjugate feedback for increasing values of the external-cavity time delay. Figure 1(a) shows self-pulsating dynamics at a frequency equal to three times the external-cavity frequency and corresponding to the so-called ECM of harmonic 3. These dynamics are observed for a relatively short external cavity ($\theta = 476$, which corresponds to a time delay $\tau = 0.666$ ns) and a low value of the feedback rate ($\gamma = 0.012$). Such harmonic self-pulsating dynamics have recently been observed in experiment [18] where it was also confirmed that, as predicted earlier [16,17], ECMs destabilize to chaotic dynamics when increasing the time-delay value and/or the feedback rate.

Figure 1(b) shows chaotic pulsing dynamics where some pulses show an intensity much larger than the average intensity value. How many such extreme events occur can be quantified, e.g., by considering the definition of the abnormality index from oceanographic studies [22], i.e., the ratio between the pulse intensity and the average intensity of one-third among the most intense pulses. Pulses that have an abnormality factor greater than 2 (see Sec. IV for details) are arbitrarily called extreme. Such a dynamic with the occurrence of rare but intense pulses resembles qualitatively the one observed recently in experiment [21] and is observed for a longer external cavity ($\theta = 1600$ or $\tau = 2.24$ ns) and for low to moderate feedback rates (from $\gamma = 0.002$ to $\gamma = 0.05$). Section IV will focus on the definition of the abnormality index and will relate the number of extreme events to the parameters of the PCF laser system.

A further increase of the external cavity length or time delay ($\theta = 3200$ or $\tau = 4.48$ ns) and of the feedback rate ($\gamma = 0.1$) yields chaotic dynamics that typically show features of so-called low-frequency fluctuations, as can be seen in Fig. 1(c). The low-pass-filtered time trace in Fig. 1(c1) unveils the occurrence of power dropouts at randomly distributed time intervals and with an averaged time separation larger than the time delay or any other internal time scales of the laser diode. Low-frequency fluctuations therefore result in a significant increase of the low-frequency content in the rf spectrum in Fig. 1(c1). A detailed theoretical study of the low-frequency fluctuation regime can be found in [19], which confirms several recent experimental findings [20].

IV. EXTREME EVENTS

The study of extreme events requires us to define what we call an event and to identify a criterion that discriminates

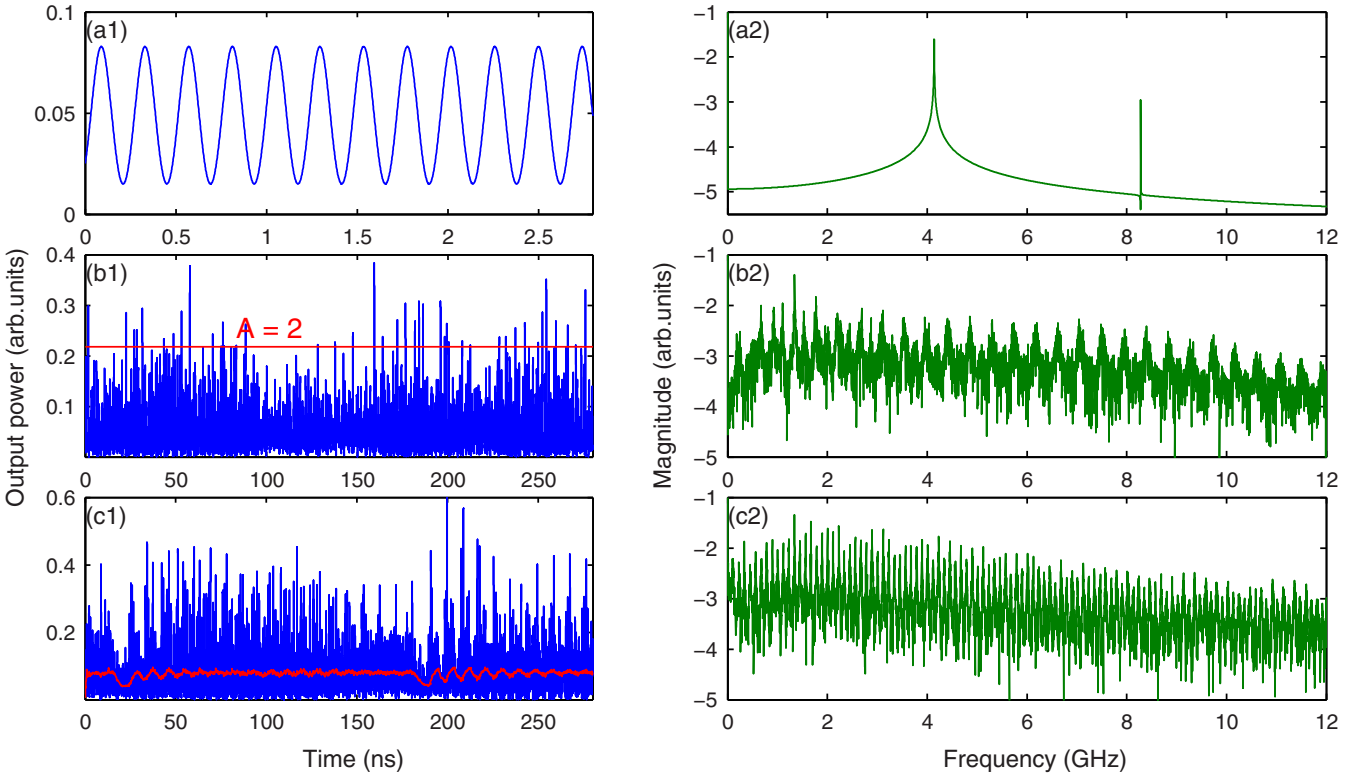

FIG. 1. (Color online) Simulated time traces (left column) and associated rf spectra (right column). (a) Unfiltered time trace of the third ECM when $\theta = 476$ and $\gamma = 0.012$. (b) Chaotic regime where we observe extreme events [peaks that overshoot the threshold $A = 2$ (see Sec. IV for details)] for $\theta = 1600$ and $\gamma = 0.025$. The associated rf spectrum shows almost no contribution in frequencies below 1 GHz. (c) Case where low-frequency fluctuations appear for $\theta = 3200$ and $\gamma = 0.1$. The low-pass-filtered trace is superimposed in gray (red) to show the power dropouts and the rf spectrum shows a significant contribution in the frequencies below 1 GHz.

what is extreme in this population. Several definitions for extreme events can be found in the literature and appear as quite arbitrary. However, as will be discussed in the following, we have checked that our conclusions and, most importantly, how the feedback strength in the PCF time-delayed system influences the occurrence and number of extreme events are robust when applying the commonly suggested criteria for extreme events.

We first discuss the definition for extreme event applied in the corresponding PCF experiment [21]. In [21] an event is defined as a local maximum of the filtered time trace of the optical output power of the laser diode. Defined for each event n is the height of the peak p_n, which is the optical output power of the local maximum. Then Hf_n, which is the difference between the peak height of the event n and the mean height of our population of events, is calculated: $Hf_n = p_n - \langle p_n \rangle_n$. Also, the significant height $H_{1/3}$ is defined as the average value among one-third of the highest values of Hf_n. Finally, the abnormality index of event n is $A_n = \frac{Hf_n}{H_{1/3}}$. Any event that yields an abnormality index greater than 2 is then considered in the following as extreme. These definitions and criteria are inspired from a proposal made to classify rogue waves in oceanographic studies [35] and have been used in several experimental and theoretical works reporting on extreme events in optics [30,36–38].

Another definition of the significant height can be inspired from a different proposal made in oceanography for the significant wave height [22], i.e., H_s is four times the standard deviation of the measured Hf_n and an event is called extreme if the corresponding abnormality index $A_n = \frac{Hf_n}{H_s} > 2$. This definition has been applied in the analysis of extreme events in the chaotic pulsing dynamics of a laser diode with optical injection [25,26]. Although we will mainly use the traditional definition of the significant height $H_{1/3}$, in the following we discuss the robustness of our conclusions against the definition of an extreme event.

A. Distribution of output power maxima

In this section and the following, we use the same external-cavity length as in the case of Fig. 1(b), $\theta = 1600$, and we vary γ from 0 to 0.05. All simulations are performed over a fixed duration of 56 μs and we observe how the number of extreme events evolves over this fixed duration. The influence on the distribution of the number of events versus their abnormality index can be clearly seen in Fig. 2. It is shown that the statistics deviate more and more from a Gaussian distribution when increasing γ. This tendency to deviate from a Gaussian distribution while increasing the driving parameter, here the feedback rate, is consistent with the experimental observations [21] and with other optical systems where extreme events or rogue waves appear when increasing, e.g., the optical pump intensity [23,28–30] or the optical injection strength [25].

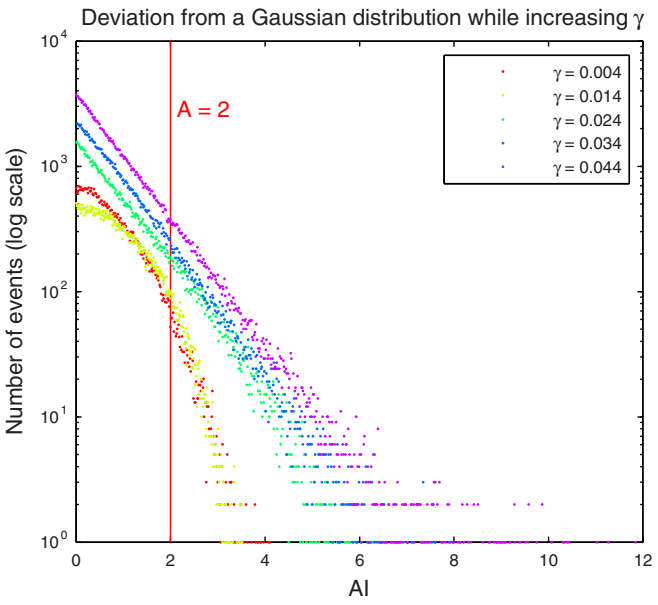

FIG. 2. (Color online) Evolution of the distribution of extreme events versus the abnormality index. Increasing the feedback rate leads to a greater deviation from a Gaussian distribution (from left to right), more extreme events, with a higher abnormality index.

Time traces of the optical output power present a strong pulsing behavior. In Fig. 3(a), where $\gamma = 0.004$, there are only a few events above the threshold $A = 2$ and Fig. 2 shows us that the most extreme one reaches only $A = 4$. In Fig. 3(b), where $\gamma = 0.024$, there are more extreme events and they

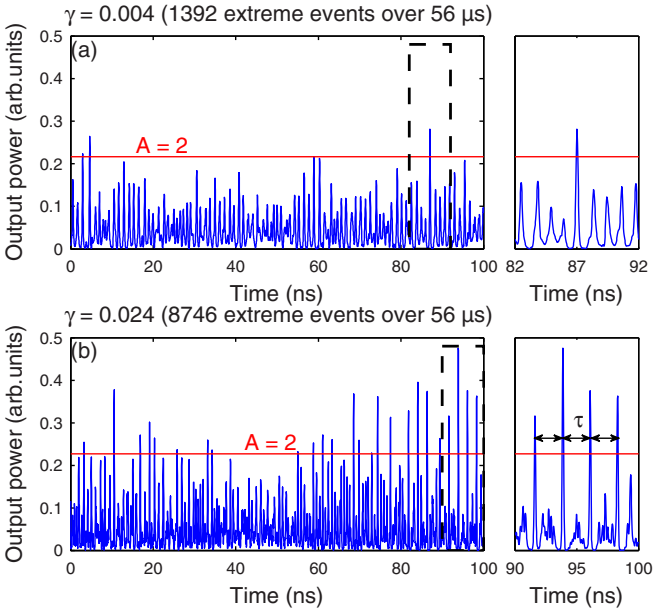

FIG. 3. (Color online) (a) and (b) Illustration of the tendency of extreme events appearing more often for strong feedback values with snapshots of the time traces where the horizontal gray (red) line indicates the threshold over which an event is considered extreme. The insets on the right show the tendency for extreme events to appear in bunches with repetitions at the time delay for several values of the feedback rate.

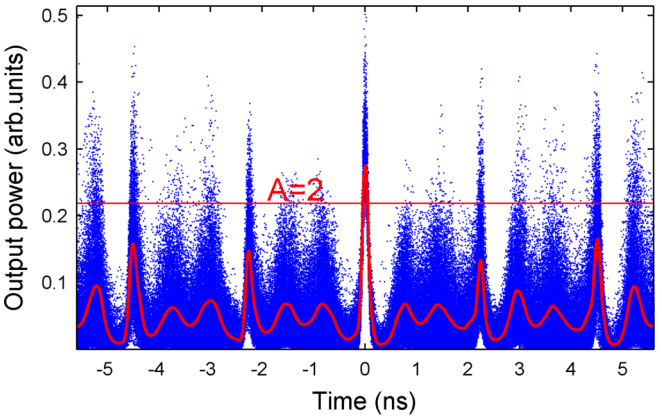

FIG. 4. (Color online) Analysis of the correlation between consecutive extreme events. Black (blue) dots are 637 time traces centered around extreme events with the largest amplitude and plotted on a 11.2-ns time window for a feedback rate $\gamma = 0.025$. The gray (red) thick line is the averaged time trace over the 637 plotted time traces.

reach high abnormality indices, some of them going above $A = 6$ according to Fig. 2. The insets on the right in Fig. 3 show an interesting feature. For low feedback rates, extreme events appear isolated, which is the expected behavior of rogue waves. However, for higher values of the feedback rate, extreme events tend to appear in bunches of pulses that repeat at a period close to the time-delay value. The bifurcation study of the PCF laser system [16,17,39,40] shows us indeed that as the feedback rate increases, the laser experiences a cascade of bifurcations. The first one is a Hopf bifurcation close to the frequency of the laser relaxation oscillations. A further increase of the feedback strength leads to a cascade of Hopf bifurcations whose frequencies are close to harmonics of the external cavity frequency, hence explaining the modulation of the laser intensity at the period of the time delay. We will classify these events in two distinct categories: Lone pulses will be named type I and bunches of pulses will be labeled type II, in agreement with the experimental observations of [21]. More specifically, through an analysis of the time separating extreme events (which is detailed in Sec. IV B), we shall consider in the following that any sequence of successive extreme events whose time separation is smaller than twice the time-delay value is called type II.

Similarly to Fig. 4 of the corresponding experiment [21], we have also analyzed the correlation properties of successive extreme events in the laser time series. For this purpose, in Fig. 4 we have superimposed 637 extreme events and centered them on a time window of 11.2 ns. In agreement with the experimental observation, successive extreme events are characterized by an extreme pulse of similar shape and duration, which is preceded and followed by pulses that are correlated and repeat at the period of the time delay, with some of these pulses also being extreme events. The pulses that repeat at the period of the external cavity therefore appear as precursors and replica of an extreme event. This property is highlighted by the red (thick) line showing the averaged time trace.

We can learn interesting facts by looking more carefully to the count of extreme events. Figure 5(a) confirms what we observed in Fig. 2: As the feedback rate increases, extreme

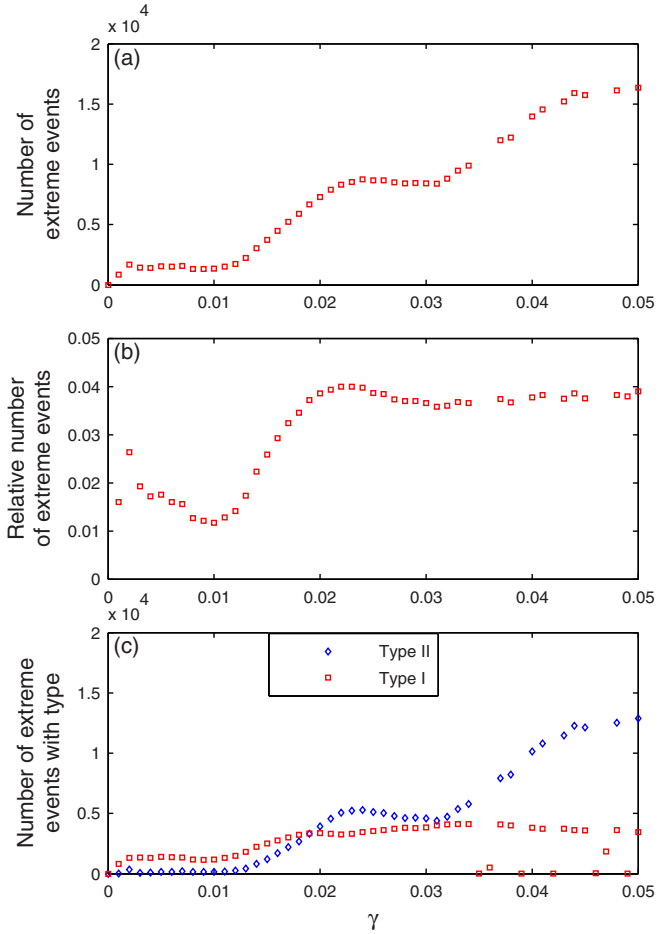

FIG. 5. (Color online) Evolution of the number of extreme events with the feedback rate: (a) absolute count over a fixed duration, (b) count relative to the total number of maxima, and (c) absolute count with distinction of types I and II.

events are more numerous, in agreement with the experimental observations of [21]. However, Fig. 5(b) shows that extreme events never represent more than 4% of the total number of events and this number saturates when further increasing the feedback rate, which is consistent with the fact that extreme events are supposed to be rare. This can be qualitatively explained by the bifurcations of the PCF laser system. Indeed, it is known theoretically that as the feedback rate increases the PCF laser system oscillates around one or several ECMs with an increasing harmonic value of the external cavity frequency. Therefore, the dynamics observed on the same time interval show a larger number of pulses and thus a larger number of events among which to count the extreme events. Both the number of events and the number of extreme events increase with the increase of feedback rate and with approximately the same rate such that the ratio of extreme events to the total number of events remains roughly the same when increasing the feedback rate. In addition, Fig. 5(c) shows that although type-I extreme events dominate for small values of the feedback rate, increasing the feedback rate leads to not only a larger proportion of type-II extreme events (bunches of pulses) but even to a majority of type-II extreme events for large values of γ.

This result agrees with the experimental observations of Ref. [21], which reported an increasing number of extreme events and a larger proportion of type-I extreme events when increasing the feedback rate. The crossing point around $\gamma = 0.02$ in Fig. 5(c) beyond which type-II extreme events dominate over type-I extreme events was not reached in the experiment, most probably due to the limited feedback strength (related to the gain of the four-wave mixing in the photorefractive crystal).

As γ increases, we saw that more extreme events are detected over the same fixed duration. This implies that they are more frequent. In the following section, we discuss how the time intervals between extreme events evolve when varying the feedback rate.

B. Time between extreme events

Experiments on a laser diode with optical feedback [21] but also on temporally driven optical speckles [29,41] suggest that the time between two successive extreme events follows a log-Poisson law. To check this feature we define t_n as the time at which the extreme event n occurs and we measure the waiting time between two consecutive extreme events on a logarithmic scale as $w_n = \ln(\frac{t_n}{t_{n-1}})$.

For low feedback rates [Fig. 6(a)], we observe that the waiting times w_n are distributed according to a log-Poisson law, which is consistent with experimental observations [21,29]. However, as also observed in experiment [21], increasing the feedback rate leads to a deviation of the statistics of the waiting times w_n from the log-Poissonian law; see Fig. 6(b). The best fitting unveils two different distributions depending on the time separation between extreme events. The law for the

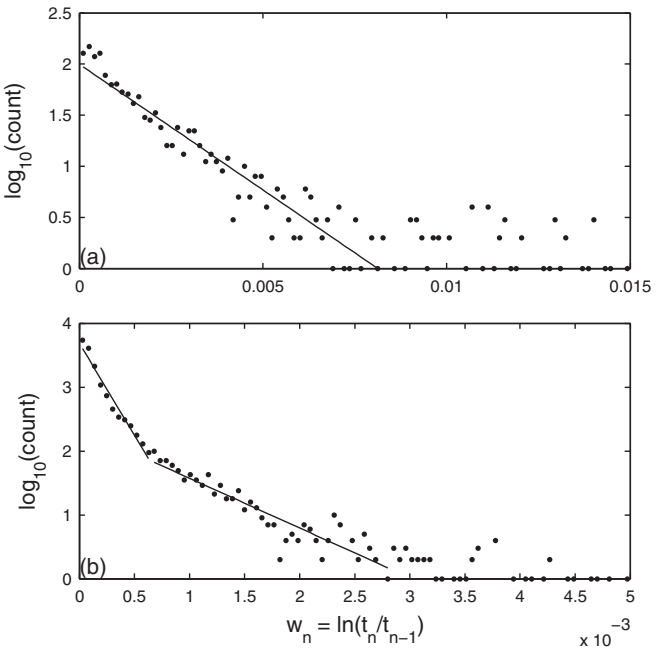

FIG. 6. Waiting times between consecutive extreme events are measured on a logarithmic scale for the cases in which (a) $\gamma = 0.004$ and the waiting-time distribution follows a log-Poisson law and (b) $\gamma = 0.044$ and waiting times are distributed according to two different log-Poisson laws.

longest waiting times represents the waiting times that would be normally observed, as in the case of a low feedback rate, while the distribution for the shortest waiting times accounts for repetitions of an extreme event at time intervals close to the time delay. Indeed, increasing the feedback rate leads to a larger number of extreme events of type II for which not only does a main pulse overshoot the threshold $A = 2$ but also the smaller pulses that repeat at a time smaller or about the value of the time delay. This yields an increasing proportion of counts of values of time separation between extreme events smaller than or close to the time-delay value, hence modifying the statistical distribution.

C. Bifurcation to extreme events

The rate-equation model reproduces qualitatively well the experimental observation of the role played by the feedback rate in modifying the number of extreme events, the type of extreme events (type I or type II), and the statistics of the time between extreme events. In this section we thus use it to provide insight into the sequence of bifurcations that yields extreme events.

Figure 7(a) shows the bifurcation diagram in the case of $\theta = 1600$ where local extrema of the filtered time traces are plotted versus the feedback rate γ. The bifurcations leading to chaotic dynamics in a PCF laser system have been analyzed in depth by several groups, including with the use of so-called continuation methods for delay-differential equations [14,16,17,39,40]. Our purpose is here to identify the parameter range where extreme events are detected and to relate these regions of extreme pulses with the sequence

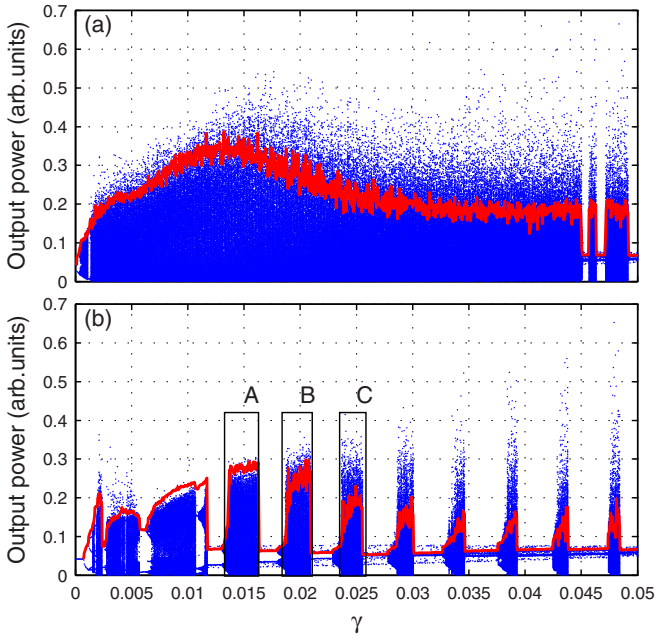

FIG. 7. (Color online) Bifurcation diagrams plotting extrema of the output power low-pass filtered at 4 GHz against the feedback rate γ for different external-cavity lengths: (a) $\theta = 476$ and (b) $\theta = 1600$. The thick (red) line is the $A = 2$ level. Extreme events seem to already appear for a short cavity. Labels A, B, and C refer to three particular bubbles of chaos on which we focus in the text and in Fig. 8.

of bifurcations leading to chaos. The evolution of the power for which $A = 2$ has also been plotted as the threshold above which we consider the intensity pulse as being extreme. This figure offers several insights. First, it confirms that extreme events are observed in a large interval of feedback rate γ that corresponds to a region of parameters leading to chaotic dynamics, as also evidenced experimentally in Ref. [21]. This chaotic dynamic appears from a sequence of period-doubling and quasiperiodic bifurcations at small feedback rates and experiences a chaos crisis at larger values of the feedback rate, leading to self-pulsating solutions called ECMs [17]. Second, this figure confirms that as the feedback rate increases, the intensity pulses exceed more and more the threshold value for extreme events, hence increasing the number of counted extreme events when increasing γ.

To clarify the role played by the ECMs, it is interesting to compare the bifurcation diagram with the one computed for a smaller value of θ, for example, $\theta = 476$ in Fig. 7(b), which corresponds to the situation analyzed theoretically in Ref. [17] and to a set of parameters used in a large number of publications analyzing in depth the bifurcation scenarios of the PCF laser system [14,16]. As γ increases, the first ECM steady state destabilizes to chaos and the laser experiences a cascade of bubbles of chaos that originate on self-pulsating (ECM) dynamics and that terminate with chaos crisis leading to other self-pulsating (ECM) dynamics of higher frequency. The chaos crisis was analyzed in detail through continuation methods in Ref. [17] and the succession of ECMs with increasing frequencies being harmonic of the external-cavity frequency was recently evidenced experimentally for the same external cavity length (leading to $\theta = 476$) [18]. This figure reveals the same conclusions on, first, the increasing number of extreme events when increasing γ and, second, on the fact that extreme events appear in parameter ranges leading to chaos and close to the onset of a chaotic crisis. The important role played by a chaotic crisis in generating extreme events was also identified theoretically in a laser diode with optical injection [26]. Still, this figure provides insight into the mechanism that is responsible for an increasing number of extreme events when increasing the feedback rate. For this purpose we look more carefully into the pulsating dynamics in three different ranges of feedback strength corresponding to the three regions labeled A, B, and C in Fig. 7(b). Figure 8 compares the pulsating dynamics (with a close-up in the right panels) for increasing values of γ, respectively, in regions A, B, and C. Two ingredients contribute to increasing the number of extreme events from Fig. 8(a) to Fig. 8(c). First, as is known in any optical feedback configuration and also identified in PCF [19], increasing the feedback strength leads to an increased level of the average output power. Figure 8 furthermore shows that not only does the averaged level of the power increase, but so does the maximum power when increasing γ. Second, a specific feature of PCF is that when increasing γ the laser bifurcates to new ECMs with increasing (harmonic) frequencies [17,18]. This is clear from Figs. 8(a2)–8(c2). Although the time duration of a pulse that reaches the extreme event threshold remains similar, the dynamics pulsate faster in Fig. 8(c2) than in Fig. 8(b2) or 8(a2) for a smaller value of γ and this is mostly visible in the time interval that separates two extreme events. This is also clear in the corresponding

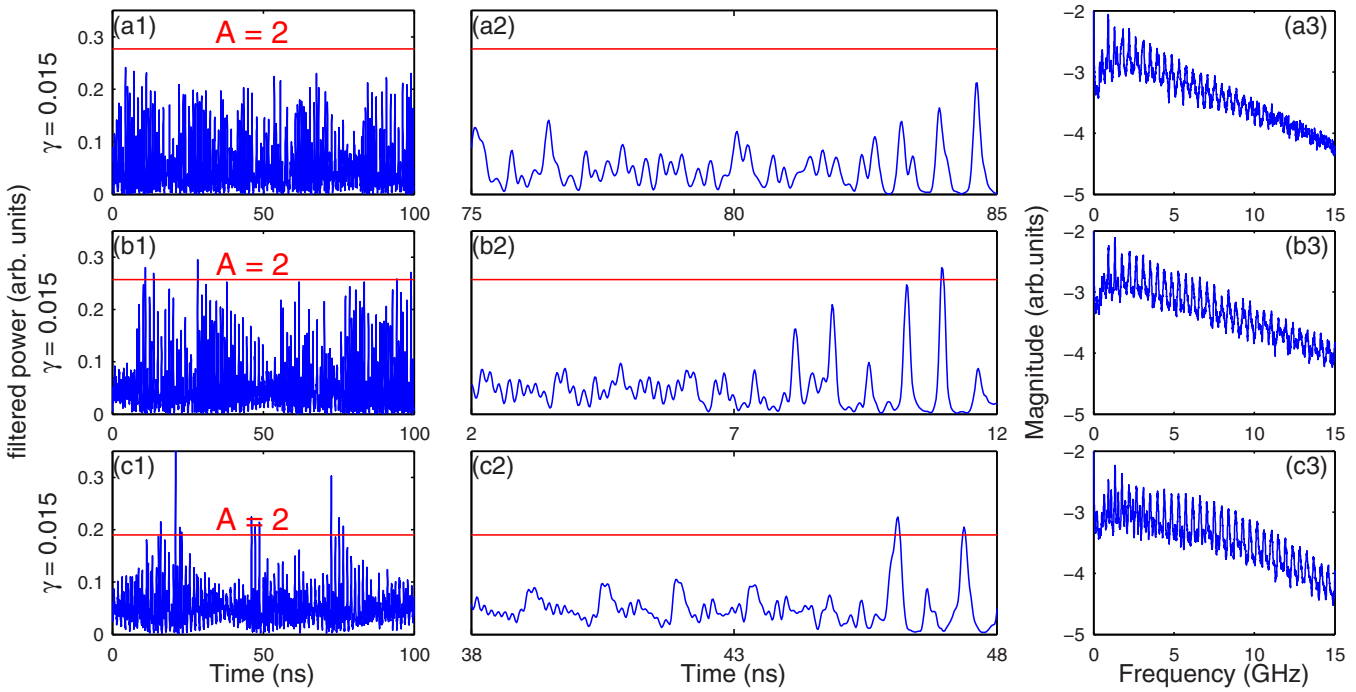

FIG. 8. (Color online) Snapshots of time traces in the case of $\theta = 476$ in three different bubbles of chaos labeled A, B, and C in Fig. 7: (a) $\gamma = 0.015$, (b) $\gamma = 0.0202$, and (c) $\gamma = 0.025$. In the left column are snapshots of 100 ns that show the evolution of the $A = 2$ level for similar waveforms. The middle column presents close-ups of those time traces that show fast oscillations close to the mean power, with a frequency that increases with the feedback rate. This increase in frequency is responsible for lowering the $A = 2$ level, thus increasing the number of extreme events detected, which can be confirmed in the right column where power spectra of the output power are plotted, showing more higher-frequency content for high feedback rates.

spectra where we identify more higher-frequency content while increasing the feedback rate. Indeed, as stated before, increasing γ means that the system has access to ECMs of higher frequencies. Because of the higher frequency in the dynamics of Fig. 8(c2), more pulses and therefore more events are counted in the same time interval in Fig. 8(c2) than in Fig. 8(b2) or 8(a2), hence contributing to decreasing the average value of the pulse intensities among one-third of the highest intensity pulses. To say this differently, this explains why the level $A = 2$ decreases with the increase of γ when comparing Figs. 8(a1), 8(a2), with Figs. 8(b1), 8(b2) and with Figs. 8(c1), 8(c2). The decreasing level of the threshold for defining an event as extreme and the larger value of the peak pulse intensity when increasing γ explain the increasing number of extreme events when increasing the feedback rate.

The conclusion drawn from Fig. 8 remains true when the criterion for an extreme event uses the definition of the significant height H_s instead of $H_{1/3}$. According to this definition, the power values corresponding to the $A = 2$ change to 0.73, 0.60, and 0.45 from Fig. 8(a) to Fig. 8(c), respectively. As mentioned before, increasing the feedback strength from Fig. 8(a) to Fig. 8(c) leads to a larger number of events corresponding to pulsing intensities with higher frequencies. Since these high-frequency pulses typically have a small amplitude around the mean value of the output power, increasing the feedback strength leads to a decreasing value of the standard deviation of recorded events, hence to a decreasing value of the $A = 2$ level and to a larger number of detected extreme events.

V. CONCLUSION

In summary, numerical simulations of a rate-equation model for a laser diode with PCF reproduce qualitatively well the experimental observations of extreme event statistics of Ref. [21]. More specifically, the three main conclusions of the experiment are captured by the model: When increasing the feedback rate (i) the deviation of the intensity statistics to the Gaussian statistics increases, leading to heavy-tailed or L -shaped statistics with a larger proportion of high-intensity pulses, as observed in general in rogue wave statistical studies [23]; (ii) the number of extreme events increases with an increasing proportion of so-called type-II extreme events that consist of extreme intensity pulses repeating at a time smaller or of the order of the time-delay value, and (iii) the statistics of the time between extreme events deviates from a log-Poissonian distribution due to the larger contribution of type-II extreme events.

Insight is gained from the bifurcation diagram over the mechanisms that underlie the increasing number of extreme events when increasing the feedback rate, i.e., on the role played by delayed feedback in generating extreme events. In particular we have identified a correlation between the increasing self-pulsating frequencies when increasing the feedback strength, which is a specific feature of PCF in contrast with COF, and the decreasing level of the extreme event threshold, hence explaining the increasing number of events counted as extreme in a statistical study.

Good agreement with all experimental observations is obtained, although the rate-equation model does not account for several features that we might think of as being important at first glance to faithfully model the setup, e.g., the nonlinear optics time scale, multiple reflections in the external cavity, and multimode laser dynamics. This demonstrates the essential role played by the two basic ingredients of the system, i.e., the phase conjugation and the time delay, in explaining the emergence of extreme events and the corresponding statistics in our system. Considering the small value of the feedback strength accessible in the PCF experiment [21] and used in the numerical simulations reported herein, we do not expect multiple reflections to significantly impact the laser dynamics and the resulting extreme event statistics. By contrast, although not well documented [33], it is expected that including the filtering effect of PCF through a finite-penetration depth nonlinear medium would lead to stabilization of the otherwise chaotic dynamics and hence would reduce the parameter range leading to extreme intensity pulses. Similarly, multimode laser dynamics are known to produce anticorrelated pulses in the modal dynamics of a laser with optical feedback [42–44], hence reducing the large intensity fluctuations in the recorded total laser intensity dynamics and the occurrence of extreme intensity pulses. Although theory and experiment agree very well qualitatively, further more quantitative agreement would require more complex investigations on the impact of the time-dependent four-wave-mixing dynamics on the chaotic, possibly multimode, laser dynamics. In addition, it is thought that this work, although concerned mostly with PCF configuration, motivates a comparison with configurations of delayed optical feedback other than PCF, in particular COF and incoherent feedback.

ACKNOWLEDGMENTS

The authors acknowledge support from Conseil Régional de Lorraine, BELSPO (Belgium) through Grant No. IAP P7/35, ANR-TINO Project No. ANR-12-JS03-005. FEDER through the project PHOTON.

[1] G. H. M. van Tartwijk and D. Lenstra, Quantum Semiclass. Opt. **7**, 87 (1995).
[2] A. Tager and K. Petermann, IEEE J. Quantum Electron. **30**, 1553 (1994).
[3] D. Lenstra, B. Verbeek, and A. Den Boef, IEEE J. Quantum Electron. **21**, 674 (1985).
[4] C. Risch and C. Voumard, J. Appl. Phys. **48**, 2083 (1977).
[5] T. Sano, Phys. Rev. A **50**, 2719 (1994).
[6] M. Sciamanna, T. Erneux, F. Rogister, O. Deparis, P. Mégret, and M. Blondel, Phys. Rev. A **65**, 041801 (2002).
[7] O. Ushakov, S. Bauer, O. Brox, H.-J. Wünsche, and F. Henneberger, Phys. Rev. Lett. **92**, 043902 (2004).
[8] T. Heil, I. Fischer, W. Elsasser, and A. Gavrielides, Phys. Rev. Lett. **87**, 243901 (2001).
[9] A. Tabaka, K. Panajotov, I. Veretennicoff, and M. Sciamanna, Phys. Rev. E **70**, 036211 (2004).
[10] F.-Y. Lin and J.-M. Liu, IEEE J. Quantum Electron. **39**, 562 (2003).
[11] L. Larger, P.-A. Lacourt, S. Poinsot, and M. Hanna, Phys. Rev. Lett. **95**, 043903 (2005).
[12] J. Saucedo Solorio, D. Sukow, D. Hicks, and A. Gavrielides, Opt. Commun. **214**, 327 (2002).
[13] G. P. Agrawal and J. T. Klaus, Opt. Lett. **16**, 1325 (1991).
[14] B. Krauskopf, G. R. Gray, and D. Lenstra, Phys. Rev. E **58**, 7190 (1998).
[15] J. S. Lawrence and D. M. Kane, Phys. Rev. A **63**, 033805 (2001).
[16] T. Erneux, A. Gavrielides, K. Green, and B. Krauskopf, Phys. Rev. E **68**, 066205 (2003).
[17] M. Virte, A. Karsaklian Dal Bosco, D. Wolfersberger, and M. Sciamanna, Phys. Rev. A **84**, 043836 (2011).
[18] A. Karsaklian Dal Bosco, D. Wolfersberger, and M. Sciamanna, Appl. Phys. Lett. **105**, 081101 (2014).
[19] E. Mercier, D. Wolfersberger, and M. Sciamanna, Opt. Lett. **39**, 4021 (2014).
[20] A. Karsaklian Dal Bosco, D. Wolfersberger, and M. Sciamanna, Europhys. Lett. **101**, 24001 (2013).
[21] A. Karsaklian Dal Bosco, D. Wolfersberger, and M. Sciamanna, Opt. Lett. **38**, 703 (2013).
[22] K. Dysthe, H. E. Krogstad, and P. Müller, Annu. Rev. Fluid Mech. **40**, 287 (2008).
[23] D. R. Solli, C. Ropers, P. Koonath, and B. Jalali, Nature (London) **450**, 1054 (2007).
[24] H. L. D. de S. Cavalcante, M. Oriá, D. Sornette, E. Ott, and D. J. Gauthier, Phys. Rev. Lett. **111**, 198701 (2013).
[25] C. Bonatto, M. Feyereisen, S. Barland, M. Giudici, C. Masoller, J. R. R. Leite, and J. R. Tredicce, Phys. Rev. Lett. **107**, 053901 (2011).
[26] J. Zamora-Munt, B. Garbin, S. Barland, M. Giudici, J. R. R. Leite, C. Masoller, and J. R. Tredicce, Phys. Rev. A **87**, 035802 (2013).
[27] J. A. Reinoso, J. Zamora-Munt, and C. Masoller, Phys. Rev. E **87**, 062913 (2013).
[28] A. Montina, U. Bortolozzo, S. Residori, and F. T. Arecchi, Phys. Rev. Lett. **103**, 173901 (2009).
[29] S. Residori, U. Bortolozzo, A. Montina, F. Lenzini, and F. T. Arecchi, Fluct. Noise Lett. **11**, 1240014 (2012).
[30] N. Marsal, V. Caullet, D. Wolfersberger, and M. Sciamanna, Opt. Lett. **39**, 3690 (2014).
[31] R. Lang and K. Kobayashi, IEEE J. Quantum Electron. **16**, 347 (1980).
[32] M. Cronin-Golomb, B. Fischer, J. O. White, and A. Yariv, Appl. Phys. Lett. **42**, 919 (1983).
[33] D. DeTienne, G. Gray, G. Agrawal, and D. Lenstra, IEEE J. Quantum Electron. **33**, 838 (1997).
[34] G. R. Gray, D. Huang, and G. P. Agrawal, Phys. Rev. A **49**, 2096 (1994).
[35] C. Kharif, E. Pelinovsky, and A. Slunyaev, in *Rogue Waves in the Ocean*, edited by K. Hutter, Advances in Geophysical and Environmental Mechanics and Mathematics Vol. 14 (Springer, Berlin, 2009).
[36] C. Lecaplain, P. Grelu, J. M. Soto-Crespo, and N. Akhmediev, Phys. Rev. Lett. **108**, 233901 (2012).

[37] A. Zaviyalov, O. Egorov, R. Iliew, and F. Lederer, Phys. Rev. A **85**, 013828 (2012).
[38] J. M. Dudley, F. Dias, M. Erkintalo, and G. Genty, Nat. Photon. **8**, 755 (2014).
[39] K. Green and B. Krauskopf, Phys. Rev. E **66**, 016220 (2002).
[40] K. Green and B. Krauskopf, Opt. Commun. **231**, 383 (2004).
[41] F. T. Arecchi, U. Bortolozzo, A. Montina, and S. Residori, Phys. Rev. Lett. **106**, 153901 (2011).
[42] P. Mandel, E. Viktorov, C. Masoller, and M. Torre, Physica A **327**, 129 (2003).
[43] M. Sciamanna, C. Masoller, F. Rogister, P. Mégret, N. B. Abraham, and M. Blondel, Phys. Rev. A **68**, 015805 (2003).
[44] I. Wallace, D. Yu, R. G. Harrison, and A. Gavrielides, J. Opt. B **2**, 447 (2000).